Trans-synaptic SynCAM Interactions in the Specification of Thalamocortical Synapses

Arda Kipcak
Charlottesville Virginia

Previous degree
Bachelor of Science (B.Sc.) in Genetics and Bioengineering,
Izmir University of Economics, 2017

A Thesis presented to the Graduate Faculty
of the University of Virginia in Candidacy for the Degree of
Master of Arts

Department of Psychology

University of Virginia
August 2023

Committee Member Names
Adema Ribic, PhD
Alev Erisir, MD, PhD

Trans-synaptic SynCAM Interactions in the Specification of Thalamocortical Synapses

Arda Kipcak[1,2,3,*]
[1] Department of Psychology, University of Virginia, VA 22903, USA
[2] Program in Fundamental Neuroscience, University of Virginia, VA 22903, USA
[3] Systems and Behavioral Neuroscience Program, University of Virginia, VA 22903, USA
[*] Correspondence: fsu3yn@virginia.edu (A.K)

SUMMARY

Cell adhesion proteins guide the development and maturation of neuronal connections by interacting across the synapse. Many adhesion molecules including SynCAM 1 have been implicated in Autism Spectrum Disorder (ASD) which shows sensory processing abnormalities tied to altered thalamocortical connectivity. Moreover, SynCAM 1 knockout mice present impaired thalamocortical connectivity. SynCAM 1 and -2 form transsynaptic complexes to promote excitatory synaptogenesis and synapse stabilization, yet their role in establishing thalamocortical connections is not understood. Here, we show that (1) *in vivo* SynCAM 1-2 interaction is more abundant than SynCAM 1-1 interaction in primary visual cortex V1. (2) SynCAM 1 and -2 expression is experience dependent as dark-reared mice had decreased SynCAM 1 and 2 (3) Silencing of SynCAM 1 at eye opening is sufficient to selectively reduce the number of thalamocortical afferents in V1 without effecting intracortical terminals and (4) ASD-linked SynCAM 1^{Y251S} mutation destabilize the protein *in silico* which in turn might contribute to its interaction efficacy. Altogether, our results indicate that SynCAM 1-2 are crucial in the establishment of thalamocortical connectivity.

INTRODUCTION

Healthy functioning of the brain critically depends on the ability of neurons to identify correct synaptic targets, form contact points (synapses) with them and maintain those synapses throughout life if needed. Although earlier steps of circuit assembly, such as axonal guidance, are relatively well-described, it is still unknown how different types of synapses are established and maintained. This is important as abnormalities in synaptic connectivity are prevalent in neurodevelopmental disorders, such as autism spectrum disorder (ASD). Mutations in genes that promote synapse formation are frequently found in ASD patients, with select abnormalities in the synaptic connectivity and function of cortical, fast spiking, parvalbumin interneurons (Anderson et al., 2012; Filice et al., 2020; Gandawijaya et al., 2021). Synaptic cell adhesion molecule 1 (SynCAM 1) is a member of a large group of proteins that organize synapses throughout the nervous system. SynCAM 1 is found exclusively in excitatory synapses (Loh et al., 2016) and promotes synapse formation via forming homo- or heterophilic transsynaptic bridges (Fogel et al., 2007, 2010). Mutations in SynCAM 1 are found in patients with ASD (Zhiling et al., 2008) and mice lacking SynCAM 1 show a marked reduction of thalamocortical inputs onto Parvalbumin^{+} inhibitory interneurons in the visual cortex. However, local excitatory inputs onto PV interneurons are unaffected by the loss of SynCAM 1, indicating that SynCAM 1 specifies thalamocortical inputs onto PV interneurons.

SynCAM 1 expression increases in the mouse visual cortex during postnatal development until the peak of critical period (~P28) (Ribic et al., 2019) when extensive synaptic remodeling takes place. Among the 4 SynCAM proteins, SynCAM 1 and -2 preferentially assemble into heterophilic complexes that were shown to promote the formation of functional synapses *in vitro* (Fogel et al., 2011). Further, loss of SynCAM 2 also results in a reduction of thalamocortical inputs onto PV^{+} interneurons (unpublished), suggesting that SynCAM1-2 interaction specifies TC→PV inputs *in vivo*. However, this has not yet been addressed. In this study, first we sought to determine the abundance of SynCAM 1-1 vs 1-2 interactions in mouse V1. As hypothesized, SynCAM 1-2 interactions was enriched in comparison to 1-1 interactions. To assess whether their expression is dependent on prior visual experience, we quantified SynCAM 1 and SynCAM 2 levels along with local and thalamic excitatory synapse markers in dark-reared and normally-reared animals. Results showed that the dark-reared animals have significantly less SynCAM 1 and -2 in visual cortex relative to normally-reared controls, confirming an experience-dependent pattern of expression. To address the role of SynCAM 1 in establishing thalamocortical connections, we carried out a conditional silencing strategy and demonstrated that the cortical knockout

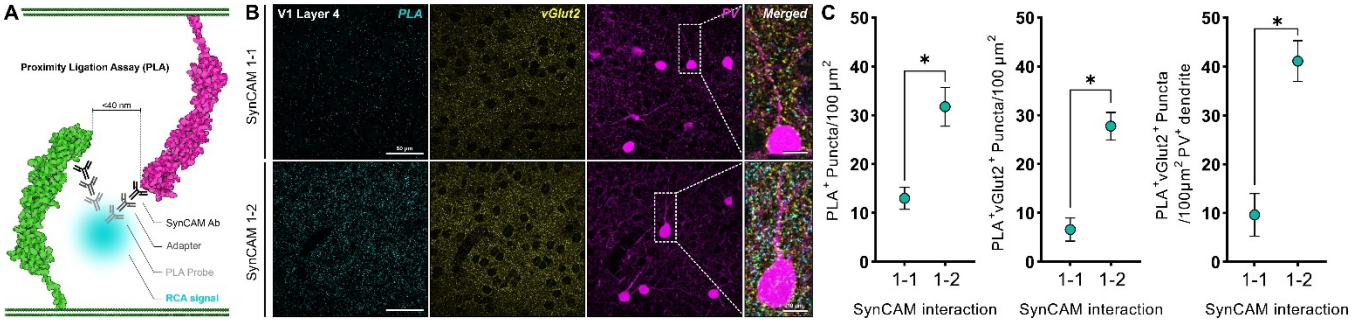

Figure 1. SynCAM 1-2 interaction is more abundant then SynCAM 1-1 interaction in V1

(A) Proximity Ligation Assay works by antibody-based detection of 2 interaction partners followed by oligo-conjugated probe attachment. Probes hybridize if the partners are in proximity and Rolling Circle Amplification (RCA, cyan) is performed *in situ* with fluorophore-attached nucleotides. Signal is detected as a distinct punctum visualized by confocal imaging.

(B) Representative images showing SynCAM interaction (PLA, cyan), vGlut2 (yellow) and PV (magenta) in Layer IV of V1.

(C) Quantification of overall (Left), vGlut2-colozalized (Middle) and vGlut2-colozalized PV dendrite-restricted (Right) PLA signal. Nested t-test $N_{1\text{-}1}$=3 mice, $N_{1\text{-}2}$=2 mice

of SynCAM 1 at P14 causes a marked reduction in thalamocortical excitatory inputs onto PV cells at V1, with no detectable change in intracortical excitatory inputs. Finally, since SynCAM 1 is found to be mutated in ASD patients, we sought to explore the effects of a detected mutation on protein structure. *In silico* analysis indicated that SynCAM 1^{Y251S} mutation destabilize the protein which may result with impaired synaptic interactions.

RESULTS

SynCAM 1-2 interaction is enriched in V1

SynCAM 1 forms homo- and heterophilic complexes with other SynCAM 1 and SynCAM 2s to promote functional synapses via increasing the number of active presynaptic terminals and enhancing excitatory transmission (Fogel et al., 2007). In rat forebrain membrane preparations, SynCAM 1 binding to SynCAM 2 was shown to be stronger than the homophilic interaction of either of them alone, but this was not tested in mouse visual cortex. To this end, we performed *in situ* proximity ligation assay (PLA) (Figure 1A) for SynCAM 1 and 2 coupled to immunohistochemistry in V1 Layer IV. Normally-reared WT mice were perfused at P28 and PLA was carried out to detect SynCAM 1-1 and 1-2 interactions. Subsequently, dual immunofluorescent labeling was done for parvalbumin and synaptic marker vGlut2. In line with previous findings by Fogel *et al.*, (2007), overall SynCAM 1-2 interaction was significantly more abundant then SynCAM 1-1 interaction in Layer IV of V1 (Nested t-test 121% Increase p<0.02 N=3 NR: 14.21±0.80; N=2 DR: 31.16±1.86 ±S.E.M.) (Figure 1C). Furthermore, SynCAM 1-2 puncta colocalized to vGlut2 puncta was also significantly higher than SynCAM 1-1 puncta overall (Nested t-test 238% Increase p<0.01 N=3 NR: 8.00±0.86; N=2 DR: 27.34±1.95 ±S.E.M.). PV+ cell dendrites was traced and used as ROIs to determine the vGlut2-colocalized axo-dendritic synapses onto PV cells. SynCAM 1-2 interaction was again more abundant that SynCAM 1-1 (Nested t-test 186% Increase p<0.01 N=3 NR: 13.84±1.12; N=2 DR: 39.82±2.25 ±S.E.M.). Taken together, this suggests that SynCAM 1-2 complex may be playing a more central role in synapse organization as opposed to their homophilic complexes.

Dark-reared mice have decreased SynCAM 1 and -2 in V1

Early life abnormal visual experience alters the structure and function of visual cortex. Visual critical period allows for a robust shift in ocular dominance (OD) in binocular V1 upon monocular deprivation, highlighting the key role of visual experience in early development. Following the closure of critical period, changes in OD and acuity is no longer reversible (Wiesel & Hubel, 1963). Dark rearing as an early-life abnormal visual experience paradigm is known to delay the maturation of visual cortex development by prolonging the critical period (Cynader & Mitchell, 1980; Fagiolini et al., 1994). SynCAM 1 is a key regulator of visual critical period plasticity and knockdown of SynCAM 1 is reinstates juvenile-like plasticity even post-critical period (Ribic, 2020). Previous work showed that SynCAM 1 expression peaks at P28 (heightened plasticity) and remains the same through adulthood (Ribic, 2020) in WT mice kept under regular light/dark cycle (12h/12h). Thus, we asked if visual deprivation by dark rearing has any effect on SynCAM expression. To investigate the effects of dark rearing, WT breeding cages were placed under 24h dark cycle. Pups were delivered and kept in dark until sacrifice with ad libitum access to food and water (Figure 1A). At P28 (the peak of critical period plasticity) litters were transcardially perfused in dark (under red light) and brains were extracted for immunohistochemistry. Dark-reared mice showed a significant reduction in SynCAM 2

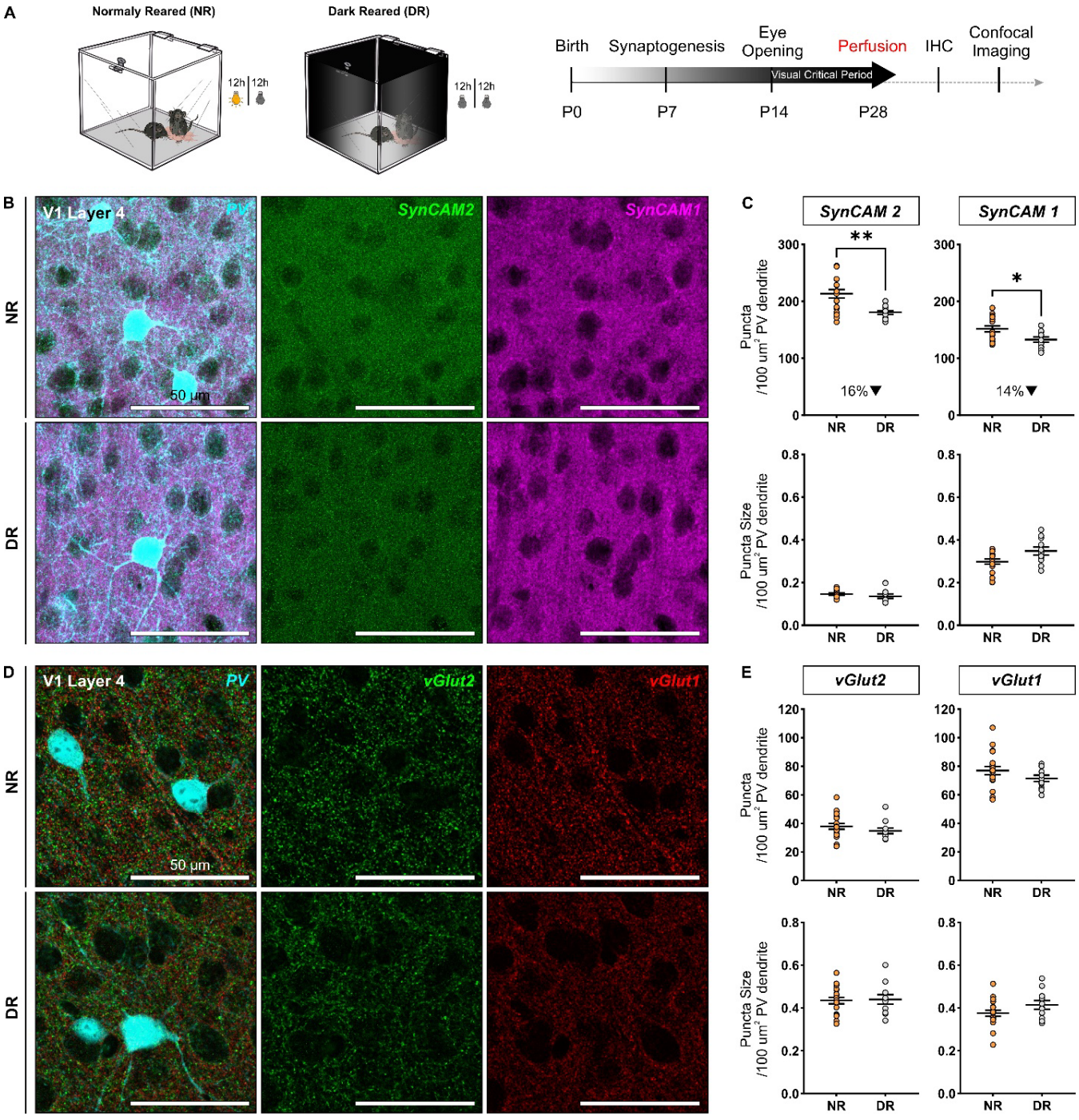

Figure 2. Dark-Rearing decreases SynCAM 1 and -2 levels without changing local and TC excitatory synapse density
(A) Left: Normal (NR) and Dark-Rearing (DR) paradigm. Right Experimental timeline. (IHC: immunohistochemistry)
(B) Fluorescent labeling of SynCAM1 (magenta) and SynCAM 2 (green) in V1 Layer IV of NR and DR mice.
(C) Quantification of SynCAM 1 and SynCAM 2 puncta density and size. Nested t-test: N_{NR}=19 mice, N_{DR}=11 mice.
(D) Fluorescent labeling of vGlut2+ (green) and vGlut1+ (red) terminals in V1 Layer IV of NR and DR mice.
(E) Quantification of vGlut2+ and vGlut1+ puncta density and size. N_{NR}=18 mice, N_{DR}=11 mice.

expression relative to normally-reared controls in Layer 4 of V1 (Welch's t test p=0.0012 16% Reduction N=18 NR: 189.8±7.5 S.E.M; N=11 DR: 159.4±3.5 S.E.M.). Parvalbumin cell dendrites outlined by IHC against PV were traced and

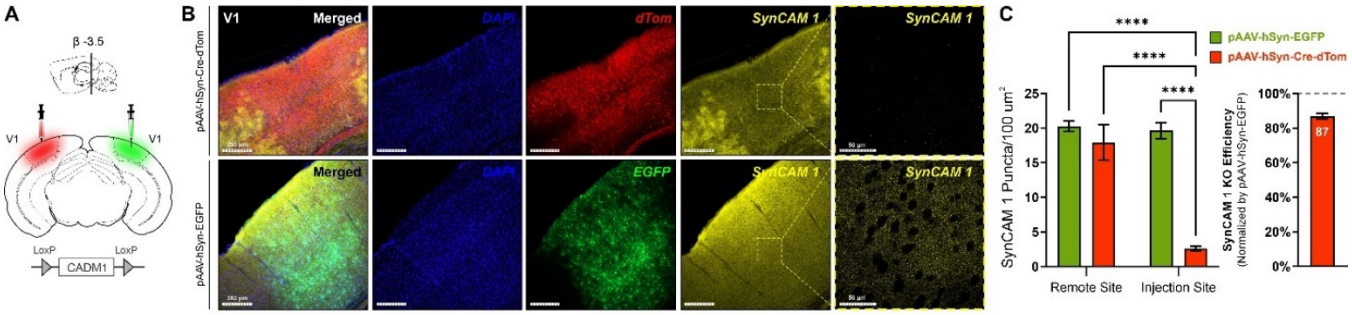

Figure 3. Cre-lox mediated conditional knockout of SynCAM 1 in V1
(A) CADM1-LoxP mice were injected with Cre or EGFP (CTR) expressing AAVs to verify SynCAM 1 knockout.
(B) Fluorescent labeling of SynCAM1 (yellow), Cre (dTom), CTR (EGFP) and cell nuclei (DAPI) at V1.
(C) Right: Quantification of SynCAM 1 puncta upon Cre vs EGFP groups at injection site and remote site. 2-way ANOVA, Tukey's Post-hoc N_{EGFP}=2, N_{Cre}=2. Left: SynCAM 1 knockout efficiency reported as %EGFP Puncta density (100 um²).

used as ROIs to determine the SynCAM 1 and SynCAM 2 abundance on PV dendrites. Compared to normally-reared animals, Dark-reared mice showed a significant reduction in PV dendrite-restricted SynCAM 1 and -2 puncta density (Figure 2B-C) (Nested t test SynCAM 1 p=0.01 14% Reduction N=18 NR: 155.1±1.4 S.E.M; N=11 DR: 135.3±1.7 S.E.M. Nested t test SynCAM 2 p=0.0036 16% Reduction N=18 NR: 213.1±1.5 S.E.M; N=11 DR: 179.2±1.1 S.E.M.) There were no significant differences in puncta size in either of the SynCAMs (Nested t test SynCAM 1 p=0.16 N=18 NR: 0.299±0.005 S.E.M; N=11 DR: 0.34±0.009 S.E.M. Nested t test SynCAM 2 p=0.18 N=18 NR: 0.15±0.001 S.E.M; N=11 DR: 0.14±0.002 S.E.M.).

Previous work demonstrates that brief monocular deprivation (3-4 days) during visual critical period results with decreased thalamocortical afferents onto layer 4 of contralateral V1, however extended periods (7 days) of MD presents no difference in the density of TC terminals ls (Coleman et al., 2010; Quast et al., 2023). In our study, there was no significant change in density and size of vGlut2+ terminals (denoting thalamocortical excitatory inputs) in dark-reared (DR) mice compared to normally-reared (NR) controls (Density Nested t test p=0.55 N=19 NR: 37.47±0.50; N=11 DR: 36.53±0.57 S.E.M. Size Nested t test p=0.9996 N=19 NR: 0.44±0.008; N=11 DR: 0.42±0.008 S.E.M.) (Figure 2D-E). Similarly, vGlut1+ terminals (denoting local/intracortical excitatory inputs) also showed no statistically significant change in puncta density or size (Density Nested t test p=0.41 N=19 NR: 80.13±0.79; N=11 DR: 73.12±0.63 S.E.M. Size Nested t test p=0.074 N=19 NR: 0.36±0.004; N=11 DR: 0.41±0.006 S.E.M.), indicating that the complete external light deprivation from birth does not change the abundance of presynaptic excitatory components.

Conditional SynCAM 1 knockout results with decreased thalamocortical terminals in V1

Literature shows that compared to WT controls, SynCAM 1 knockout mice at both critical period (P28) and adulthood (P60) had fewer thalamocortical inputs onto PV interneurons in V1. Moreover, adult (P60) PV-Cre mice also had reduced vGlut2+ terminals onto PV cells after PV-specific knockdown of SynCAM 1 via P14 AAV injection in bV1 (Ribic, Crair and Biederer, 2019). To see if removal of neuronal SynCAM 1 from V1 recapitulates this effect, we injected CADM1-LoxP mice (floxed for SynCAM 1) at P14 with Cre-expressing or control AAVs. First, Cre-Lox mediated conditional knockout was verified (Figure 3A) by immunohistochemistry. Animals were injected with Cre or EGFP viruses in V1 and SynCAM 1 puncta was quantified. As expected, Cre injection resulted with a marked reduction in SynCAM 1 puncta relative to EGFP injections at injection site (2-way ANOVA, Tukey's Post-hoc 87% Reduction p<0.0001 N=2/group Mean difference in puncta density: EGFP vs Cre 20.12±0.9 ±S.E.M.). To account for any potential regional variabilities in SynCAM 1 expression, knockout efficiency was also verified by quantifying the SynCAM 1 at a remote site (A1, not shown) away from injection (Figure 3C). Overall, >80% knockout efficiency was achieved.

To test the hypothesis that removal of SynCAM 1 in V1 will result with decreased TC inputs, CADM1-LoxP animals were injected with Cre expressing (AAV-hSyn-Cre-dTom) or control (AAV-hSyn-TurboRFP) viruses in V1 at eye opening (P14) and sacrificed at critical period closure (P35). Brains were sectioned and immunohistochemistry was performed by dual labeling for vGlut1 and vGlut2. As hypothesized, there was a significant reduction in the number of vGlut2+ terminals imaged at Layer IV of V1 (Nested t test 21% Reduction p=0.034 N=19 RFP: 55.2±1.32; N=11 Cre: 43.53±2.48 S.E.M.) and no change in puncta size (Figure 4C-D) (Nested t test p=0.596 N=19 RFP: 0.26±0.00798; N=11 Cre: 0.29±0.016 S.E.M.). There was no change in the density or

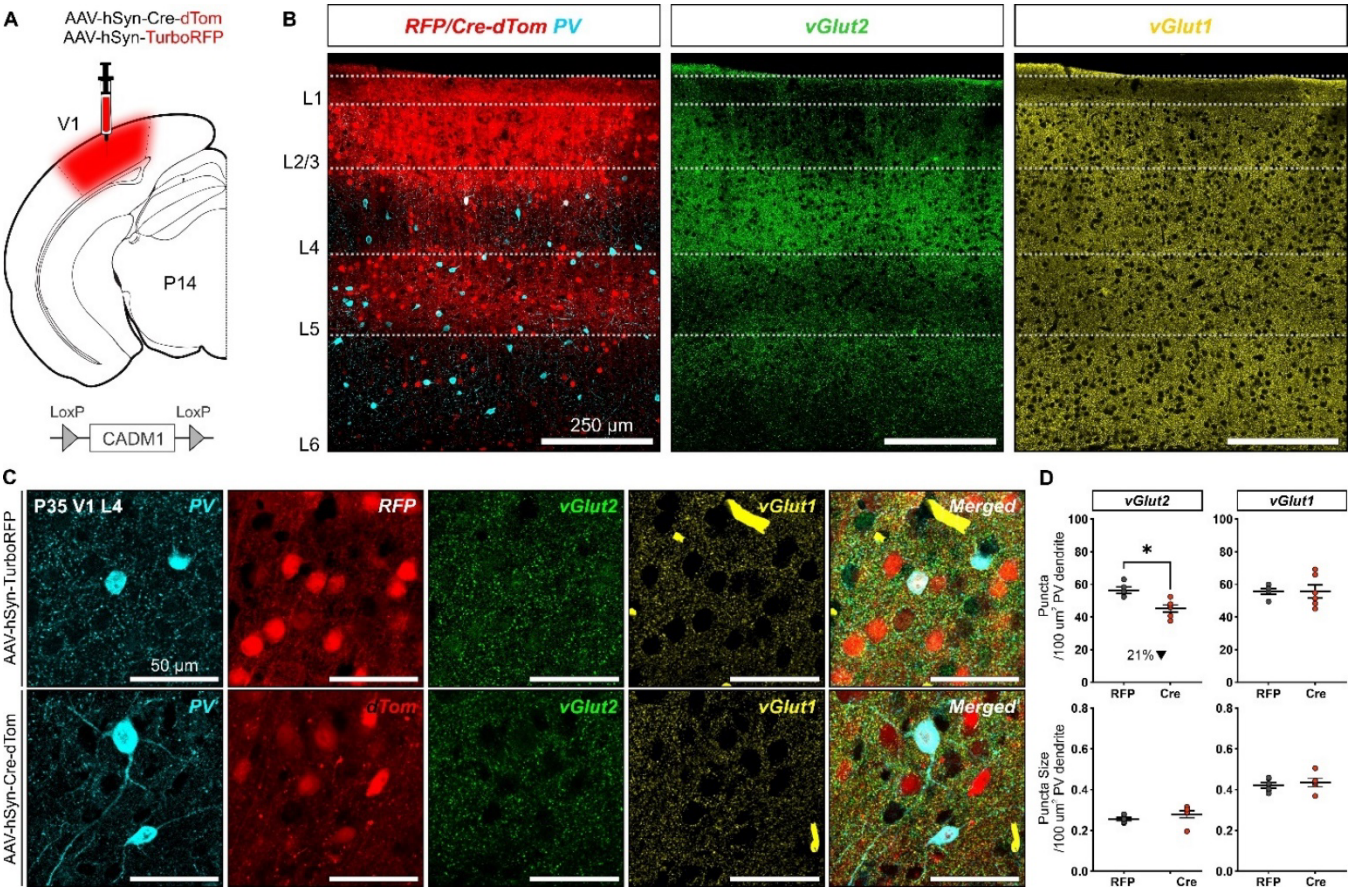

Figure 4. Conditional knockout of SynCAM 1 results with decreased thalamocortical inputs in V1
(A) CADM1-loxP mice were injected with Cre expressing or control (RFP) AAVs in V1 at P14 (eye opening) and sacrificed at P35 (critical period closure).
(B) Representative images of dual labeling of vGlut2+ and vGlut1+ terminals in V1 Layer I-VI at P35 in animals injected with Cre or RFP expressing AAVs. Thalamorecipient Layer (IV) is easily distinguishable by the thick vGlut2 staining (middle) in contrast to vGlut1 which is distributed more homogeneously throughout the layers.
(C) Representative images showing an example PV neuron infected by the respective AAVs.
(D) Quantification of vGlut2+ (left) and vGlut1+ (right) puncta density and size in RFP vs Cre injected groups Non-parametric t-test N_{RFP}=19, N_{Cre}=11.

size of vGlut1+ puncta (Density Nested t test p=0.45 N=19 CTR: 55.13±2.12; N=11 Cre: 51.83±2.56 S.E.M. Size Nested t test 19% Reduction p=0.81 N=19 CTR: 0.42±0.02; N=11 Cre: 0.42±0.026 S.E.M.). Together, this shows that conditional removal of SynCAM 1 at P14 is sufficient to selectively impair the thalamocortical structural connectivity in V1, without effecting the intracortical excitatory terminals.

ASD-linked Y251S mutation is potentially destabilizing SynCAM 1

Many neurodevelopmental conditions, especially Autism Spectrum Disorder (ASD) have long been associated with mutations in genes encoding for cell adhesion molecules due to their key roles in mediating synaptic connectivity (Stewart, 2015; Eve *et al.*, 2022). Mutations in CADM1 (encoding SynCAM 1) has also been previously implicated in ASD (Zhiling *et al.*, 2008; Fujita *et al.*, 2010). Among 2 familial ASD mutations in CADM1 reported by Zhiling *et al.*, (2008), Tyrosine to Serine conversion at position 251 (referred to as Y251S) was of particular interest to the project. This amino acid change is due to a point mutation (A774C substitution), changing TAT codon to TCT codon, resulting with the translation of the smaller amino acid Serine instead of the bulkier Tyrosine. Fujita *et al.*, (2010) showed that SynCAM^{Y251S}-expressing primary neurons possessed morphological abnormalities with shorter dendrites and impaired synaptogenesis *in vitro*. They also report that SynCAM^{Y251S} had slightly reduced homophilic binding

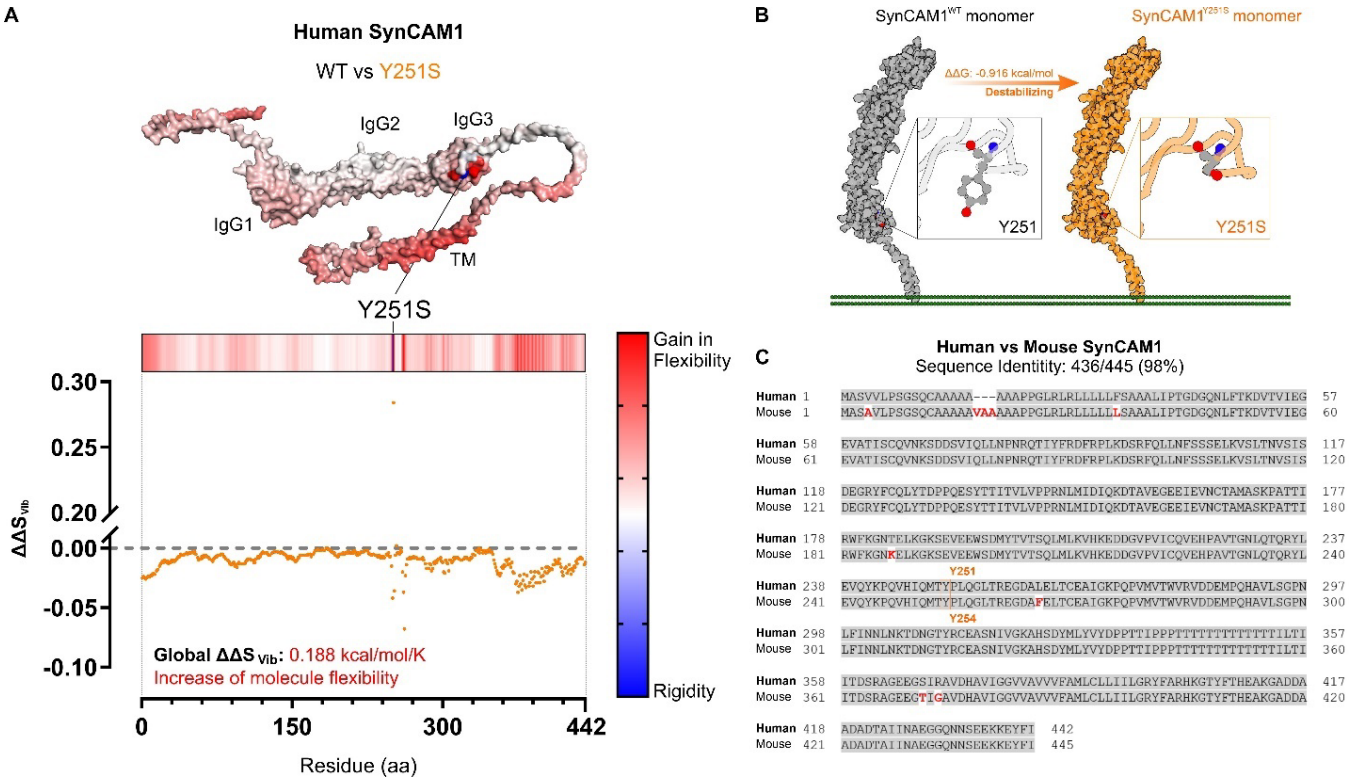

Figure 5. SynCAM1^{Y251S} mutation destabilizes the monomer by increasing its flexibility *in silico*
(A) 3D Structure of SynCAM1^{Y251S} showing regions with change in flexibility (red: increased, blue: decreased). $\Delta\Delta S_{Vib}$: Vibrational Entropy Energy in kcal/mol/K. X-axis showing residues of full length human SynCAM 1 (Isoform D) from aa 1-442.
(B) Representative image showing close-up view of the location of the mutation and the change in amino acid structure.
(C) Amino acid sequence alignment of human vs mouse SynCAM 1. Orange box shows the conserved Tyrosine residue that is mutated (see methods for details).

capabilities, however it's heterophilic interactions with SynCAM 2 was never assessed as well as any other possible effects *in vivo.* ASD-linked SynCAM 1 mutation is located in the third Ig domain (Y251S) which is essential for lateral cis-assembly with other SynCAM 1s and facilitate heterophilic binding to SynCAM 2 (Fogel *et al.*, 2010). As PV-expressed SynCAM 1 is necessary for proper function of TC circuits, the working hypothesis is that Y251S mutation impairs the transsynaptic SynCAM 1-2 interaction and results in ASD-linked sensory processing abnormalities. For this purpose, we first evaluated the effects of this mutation on 3D structure of human SynCAM 1 *in silico.* As shown in Figure 5A, SynCAM1^{Y251S} had an overall increase in Vibrational Entropy. Energy ($\Delta\Delta S_{Vib}$ = 0.188 kcal/mol/K) and an increase in Gibbs free energy change (ΔΔG=0.916 kcal/mol) (Figure 5B). ΔΔG denotes the difference in change in energy between the unfolded vs folded state between the WT and mutant polypeptide. As the ΔΔG reflects the thermodynamic stability of the mutant protein in relation to WT protein ΔΔG of 0.916 kcal/mol of SynCAM1^{Y251S} predicts destabilization in the 3D structure of the protein due to a gain in flexibility.

DISCUSSION

Despite substantial research, the link between cell adhesion molecules and their role in synaptic selectivity is not well understood. Mounting evidence suggest that synaptic partner choice i.e., synapse specificity is established via certain combinations of pre- and post-synaptic cell surface expression of cell adhesion proteins during development (Sanes & Zipursky, 2020; Südhof, 2021). Results of our study show that (1) SynCAM 1-2 interaction is more abundant than SynCAM 1-1 interaction in primary visual cortex. (2) SynCAM 1 and -2 expression is experience dependent as dark-reared mice had decreased SynCAM 1 and 2 Puncta (3) Silencing of SynCAM 1 at eye opening is sufficient to selectively reduce the number of thalamocortical afferents in V1 without effecting intracortical terminals and (4) ASD-linked SynCAM 1^{Y251S}

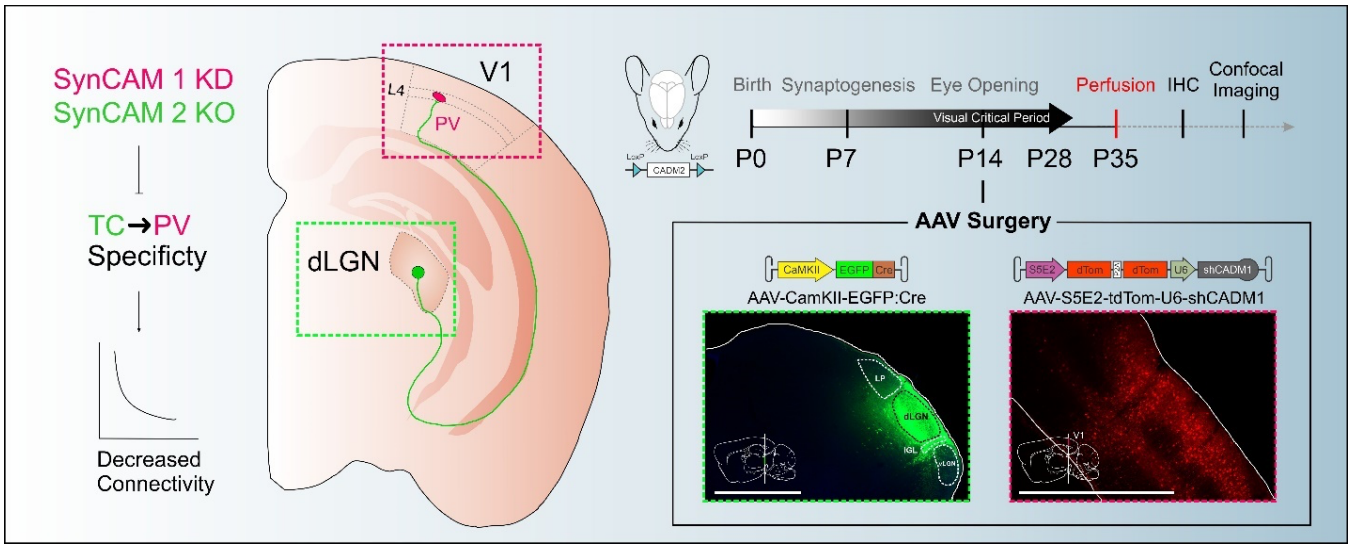

Figure 6. Future experimental design
Left: Depiction of the hypothesis. Right: Designated experimental timeline. CADM2-LoxP animals will be injected with Cre-expressing AAVs in dorsolateral Geniculate Nucleus (dLGN) and/or with shCADM1-expressing PV-specific AAVs in primary visual cortex (V1).

mutation destabilize the protein *in silico* which in turn might contribute to its interaction efficacy. Although proximity ligation is a useful tool to detect protein-protein interactions *in situ*, one limitation of the assay is that it is unable to distinguish cis vs trans-synaptic complexes. Previous literature indicates that post-synaptic (i.e., cortical) action of SynCAM 1 is the main driver of its functionality (Ribic et al., 2019; Robbins et al., 2010). Furthermore, since SynCAM 1 preferentially binds to SynCAM 2, suggestive of a pre-synaptic (i.e., thalamic) role for SynCAM 2. In this context, future direction of the study is to test this hypothesis by cell type-specific pre-, post- and transsynaptic silencing SynCAM 2 and SynCAM 1 respectively (Figure 6). To this end, we cloned a recombinant AAV that expresses shCADM1 RNAi construct with an RFP reporter in a PV cell-specific manner (Vormstein-Schneider *et al.*, 2020). Experimental design focuses on cre-lox mediated knockout of pre-synaptic (thalamic) SynCAM2 and RNAi-mediated knockdown of post-synaptic (cortical PV) SynCAM 1 i.e., transsynaptic dual silencing in the same animals and asses the TC→PV connectivity using CADM2-LoxP animals. Lastly, we plan to further investigate the effects of SynCAM^{Y251S} mutation on TC connectivity and behavior. Sequence alignment shows high degree conservation between human and mouse SynCAM 1 (Figure 5C). In particular Tyrosine (Y) residue that is implicated in human ASD is also conserved between the species. In line with this, we generated expression constructs to ectopically express mutant SynCAM 1 via intraventricular AAV injections at P0 and evaluate its effects on synaptic connectivity as well as ASD-phenotype *in vivo.* In conclusion, our preliminary findings here indicate that SynCAM 1-2 interaction may be crucial to facilitate the establishment of proper thalamocortical connectivity in the visual cortex. Although there are great steps taken in the scientific community to understand how different regions function, a great majority of the current efforts are focused extensively on clinical improvement without the sufficient understanding of underlying mechanisms. And yet, how exactly the synaptic partner selection takes place is unknown. By better understanding how developmental events in early life effect sensory processing, we can develop better strategies to target developmental problems. Ultimately, long standing goal of the proposed project is to develop a sufficiently complex understanding of synapse-level changes that generate an adhesion code and shape connectivity.

METHODS

Animals

Dark rearing paradigm was carried out using Wild type C57BL6/J mice (The Jackson Laboratory). For conditional knock-out experiments, Floxed SynCAM 1 (CADM1-LoxP) and Floxed SynCAM 2 (CADM2-Loxp) mouse lines were used. CADM1-LoxP line (Rathjen et al., 2017, p. 1) was a gift from Matthew N. Poy (Johns Hopkins) whereas CADM2-LoxP line (CSD70565) was obtained from KOMP MMRRC Repository UC Davis. Animals of both sexes were used for all experiments and had access to food and water ad libitum. All animals were kept at 12h/12h reverse light/dark cycle except the dark reared animals, which were kept at dark for 24h from birth until sacrifice. All procedures involving animals were performed in accordance with Institutional Animal Care and Use Committee (IACUC) guidelines.

Intracranial AAV Injections

Animals at P14 were anesthetized with 2% Isoflurane in anesthesia chamber with 300 ml/min flow rate for 10 minutes and then placed under nose cone with a flow rate of 100 ml/min for the duration of the surgery. AAVs injections were carried out using stereotactic coordinates: 600 nL 10^{11} vg/mL AAV-hSyn-Cre-dTom (Addgene, 107738) or AAV-hSyn-TurboRFP (Addgene, 105552) was injected to visual cortex (β, AP: -3.0; ML: 2.8, DV:0.4) or 50 nL at dLGN (β, AP: -2.5; ML: 2.1, DV: 2.9). Infusion at a rate of 0.5 nL/s was initiated right before tissue penetration to provide positive pressure and prevent clogging. Following infusion, needle was kept still for extra 5-10 minutes to allow proper tissue diffusion and prevent backflow. At experimental endpoints (indicated at figure legends) animals were transcardially perfused first with 1 M PB and then with 4% PFA. Brains were extracted and post-fixed in 4% PFA overnight followed by a wash in 1X PBS. Later, brains were embedded in 2.5% agarose in PBS and sectioned at 40 mm using vibratome (Leica VT1000). Sections were stored in 1X PBS with 0.01% sodium azide at 4°C until PLA and/or IHC experiments.

Proximity Ligation (PLA) and Immunohistochemistry (IHC)

To detect the interactions between tissue expressed SynCAMs Duolink Proximity Ligation Assay (Sigma-Aldrich, DUO92101). *In situ* Proximity Ligation assay allows fluorescent detection of endogenous protein interactions based on the proximity of the interacting partners. Briefly, heat-induced epitope retrieval (HIER) at 80C in sodium citrate was performed on 40 uM thick V1 sections followed by 1 hour blocking in 3% BSA and 0.03% Triton X-100 in PBS at room temperature. Then, primary antibody incubation with the same buffer using chicken anti-SynCAM 1 and/or mouse anti-SynCAM 2 was carried out overnight at 4C with gentle shaking. Second day, tissues were washed in 1X PBS and incubated with rabbit anti-chicken and goat anti-mouse bridging antibodies (adapters) overnight at 4C with gentle shaking. This step was added to the original protocol from the manufacturer since the PLA probes the kit provides are raised against rabbit (+probe) and mouse (-probe). Next day, tissues were washed and incubated with the probes for 60 min at 37 °C. Ligation and amplification steps were carried out as instructed by the manufacturer. Following amplification, sections were washed, and immunohistochemistry was subsequently carried out. For double and triple-labeling experiments (including PLA), IHC was done by sequential antibody incubations to prevent the formation of any leaky signal between channels. Shortly, HIER (depending on the antibody) and blocking was carried out as described above and sections were incubated with the primary antibodies overnight at 4C with gentle shaking. Following primary antibody incubations, secondary antibody incubations were done with the same method. Lastly, depending on the experiment sections were wither counterstained with DAPI and washed in 1X PBS and or directly mounted on slides in distilled water before coverslipping with mounting medium (Polysciences, 18606-20).

Confocal Microscopy and Image Analysis

Confocal microscopy was performed on a Leica Stellaris 5 or a Zeiss LSM 700 microscope. All Images used for quantification were acquired at 63X oil lens with using same settings for each group within experiments. Single optical sections were used for the quantification of all stainings (vGlut1, vGlut2, SynCAM 1, SynCAM 2). Fiji (NIH) was used for image analysis. Images were first thresholded and binarized to generate masks. Then, size and mean intensity data per individual puncta were extracted via the masks using particle analyzer. Generated datasets were imported to Prism 8 (GraphPad Software, San Diego, California USA), normality was assessed and suitable hypothesis testing and post-hoc comparisons was performed depending on the data (detailed in the individual figure and figure legends).

3D Protein Modeling of the Mutation and Visualization

Protein data bank was searched for human SynCAM 1 but no crystal structures were registered. Mouse SynCAM 4, the structurally and sequence-vise closest molecule was then assessed and selected for homology modeling using SWISS-MODEL (Waterhouse et al., 2018). Top-performer was selected among multiple models generated however because of the template coverage models (not shown here) were limited to Ig domains but not the whole peptide. Thus, a different strategy was followed: AlphaFold (Jumper et al., 2021) was searched for human SynCAM 1 models and SynCAM 1 model AF-Q9BY67 based on canonical human SynCAM 1 transcript (NCBI Ref Seq: NP_055148.3) was selected. AF-Q9BY67 was then imported into DynaMut (Rodrigues et al., 2018) and SynCAM1^{Y251S} was evaluated for its structural stability in relation to SynCAM^{WT}. Representative full-length 3D SynCAM1^{Y251S} image in Figure 5A was colored based on $\Delta\Delta S_{Vib}$/residue using PyMOL 2.0 (Schrödinger & DeLano, 2020). Representative SynCAM1 and SynCAM1^{Y251S} images at Figure 5B covers the region between res. 49-342 (IgG1-3 domains and extracellular loop upstream to TM) and was generated using Goodsell-like pseudo-coloring of The Protein Imager tool (Tomasello et al., 2020).

ACKNOWLEDGMENTS

First and foremost, I (A.K.) would like to extend my gratitude to my mentors Dr. Adema Ribic (Department of Psychology, UVA) and Dr. Alev Erisir (Department of Psychology, UVA) their continued guidance. We also thank Dr. Jess Connely and Lab members (Department of Psychology, UVA) for their technical help with cell culture as well as Dr. JC Cang (Department of Psychology, UVA) and Dr. Xiaorong Liu labs (Department of Psychology, UVA) for the use of confocal microscopy and gel documentation systems. Finally, we thank

Program in Fundamental Neuroscience for the use of Leica stellaris confocal microscope. This work was supported by NIH Startup grant, iTHRIV and University of Virginia Brain Institute.

REFERENCES

Anderson, G. R., Galfin, T., Xu, W., Aoto, J., Malenka, R. C., & Sudhof, T. C. (2012). Candidate autism gene screen identifies critical role for cell-adhesion molecule CASPR2 in dendritic arborization and spine development. *Proceedings of the National Academy of Sciences*, *109*(44), 18120–18125. https://doi.org/10.1073/pnas.1216398109

Coleman, J. E., Nahmani, M., Gavornik, J. P., Haslinger, R., Heynen, A. J., Erisir, A., & Bear, M. F. (2010). Rapid Structural Remodeling of Thalamocortical Synapses Parallels Experience-Dependent Functional Plasticity in Mouse Primary Visual Cortex. *Journal of Neuroscience*, *30*(29), 9670–9682. https://doi.org/10.1523/JNEUROSCI.1248-10.2010

Cynader, M., & Mitchell, D. E. (1980). Prolonged sensitivity to monocular deprivation in dark-reared cats. *Journal of Neurophysiology*, *43*(4), 1026–1040. https://doi.org/10.1152/jn.1980.43.4.1026

Fagiolini, M., Pizzorusso, T., Berardi, N., Domenici, L., & Maffei, L. (1994). Functional postnatal development of the rat primary visual cortex and the role of visual experience: Dark rearing and monocular deprivation. *Vision Research*, *34*(6), 709–720. https://doi.org/10.1016/0042-6989(94)90210-0

Filice, F., Janickova, L., Henzi, T., Bilella, A., & Schwaller, B. (2020). The Parvalbumin Hypothesis of Autism Spectrum Disorder. *Frontiers in Cellular Neuroscience*, *14*, 577525. https://doi.org/10.3389/fncel.2020.577525

Fogel, A. I., Akins, M. R., Krupp, A. J., Stagi, M., Stein, V., & Biederer, T. (2007). SynCAMs Organize Synapses through Heterophilic Adhesion. *Journal of Neuroscience*, *27*(46), 12516–12530. https://doi.org/10.1523/JNEUROSCI.2739-07.2007

Fogel, A. I., Li, Y., Giza, J., Wang, Q., Lam, T. T., Modis, Y., & Biederer, T. (2010). N-Glycosylation at the SynCAM (Synaptic Cell Adhesion Molecule) Immunoglobulin Interface Modulates Synaptic Adhesion. *Journal of Biological Chemistry*, *285*(45), 34864–34874. https://doi.org/10.1074/jbc.M110.120865

Fogel, A. I., Stagi, M., Perez de Arce, K., & Biederer, T. (2011). Lateral assembly of the immunoglobulin protein SynCAM 1 controls its adhesive function and instructs synapse formation. *The EMBO Journal*, *30*(23), 4728–4738. https://doi.org/10.1038/emboj.2011.336

Gandawijaya, J., Bamford, R. A., Burbach, J. P. H., & Oguro-Ando, A. (2021). Cell Adhesion Molecules Involved in Neurodevelopmental Pathways Implicated in 3p-Deletion Syndrome and Autism Spectrum Disorder. *Frontiers in Cellular Neuroscience*, *14*, 611379. https://doi.org/10.3389/fncel.2020.611379

Jumper, J., Evans, R., Pritzel, A., Green, T., Figurnov, M., Ronneberger, O., Tunyasuvunakool, K., Bates, R., Žídek, A., Potapenko, A., Bridgland, A., Meyer, C., Kohl, S. A. A., Ballard, A. J., Cowie, A., Romera-Paredes, B., Nikolov, S., Jain, R., Adler, J., … Hassabis, D. (2021). Highly accurate protein structure prediction with AlphaFold. *Nature*, *596*(7873), 583–589. https://doi.org/10.1038/s41586-021-03819-2

Loh, K. H., Stawski, P. S., Draycott, A. S., Udeshi, N. D., Lehrman, E. K., Wilton, D. K., Svinkina, T., Deerinck, T. J., Ellisman, M. H., Stevens, B., Carr, S. A., & Ting, A. Y. (2016). Proteomic Analysis of Unbounded Cellular Compartments: Synaptic Clefts. *Cell*, *166*(5), 1295-1307.e21. https://doi.org/10.1016/j.cell.2016.07.041

Quast, K. B., Reh, R. K., Caiati, M. D., Kopell, N., McCarthy, M. M., & Hensch, T. K. (2023). Rapid synaptic and gamma rhythm signature of mouse critical period plasticity. *Proceedings of the National Academy of Sciences*, *120*(2), e2123182120. https://doi.org/10.1073/pnas.2123182120

Rathjen, T., Yan, X., Kononenko, N. L., Ku, M.-C., Song, K., Ferrarese, L., Tarallo, V., Puchkov, D., Kochlamazashvili, G., Brachs, S., Varela, L., Szigeti-Buck, K., Yi, C.-X., Schriever, S. C., Tattikota, S. G., Carlo, A. S., Moroni, M., Siemens, J., Heuser, A., … Poy, M. N. (2017). Regulation of body weight and energy homeostasis by neuronal cell adhesion molecule 1. *Nature Neuroscience*, *20*(8), 1096–1103. https://doi.org/10.1038/nn.4590

Ribic, A. (2020). Stability in the Face of Change: Lifelong Experience-Dependent Plasticity in the Sensory Cortex. *Frontiers in Cellular Neuroscience*, *14*, 76. https://doi.org/10.3389/fncel.2020.00076

Ribic, A., Crair, M. C., & Biederer, T. (2019). Synapse-Selective Control of Cortical Maturation and Plasticity by Parvalbumin-Autonomous Action of SynCAM 1. *Cell Reports*, *26*(2), 381-393.e6. https://doi.org/10.1016/j.celrep.2018.12.069

Robbins, E. M., Krupp, A. J., Perez de Arce, K., Ghosh, A. K., Fogel, A. I., Boucard, A., Südhof, T. C., Stein, V., & Biederer, T. (2010). SynCAM 1 Adhesion Dynamically Regulates Synapse Number and Impacts Plasticity and Learning. *Neuron*, *68*(5), 894–906. https://doi.org/10.1016/j.neuron.2010.11.003

Rodrigues, C. H., Pires, D. E., & Ascher, D. B. (2018). DynaMut: Predicting the impact of mutations on protein conformation, flexibility and stability. *Nucleic Acids Research*, *46*(W1), W350–W355. https://doi.org/10.1093/nar/gky300

Sanes, J. R., & Zipursky, S. L. (2020). Synaptic Specificity, Recognition Molecules, and Assembly of Neural Circuits. *Cell*, *181*(3), 536–556. https://doi.org/10.1016/j.cell.2020.04.008

Schrödinger, L., & DeLano, W. (2020). *PyMOL* (2.4.0) [Computer software]. http://www.pymol.org/pymol

Südhof, T. C. (2021). The cell biology of synapse formation. *Journal of Cell Biology*, *220*(7), e202103052. https://doi.org/10.1083/jcb.202103052

Tomasello, G., Armenia, I., & Molla, G. (2020). The Protein Imager: A full-featured online molecular viewer interface with server-side HQ-rendering capabilities. *Bioinformatics*, *36*(9), 2909–2911. https://doi.org/10.1093/bioinformatics/btaa009

Waterhouse, A., Bertoni, M., Bienert, S., Studer, G., Tauriello, G., Gumienny, R., Heer, F. T., de Beer, T. A. P., Rempfer, C., Bordoli, L., Lepore, R., & Schwede, T. (2018). SWISS-MODEL: Homology modelling of protein structures and complexes. *Nucleic Acids Research*, *46*(W1), W296–W303. https://doi.org/10.1093/nar/gky427

Wiesel, T. N., & Hubel, D. H. (1963). SINGLE-CELL RESPONSES IN STRIATE CORTEX OF KITTENS DEPRIVED OF VISION IN ONE EYE. *Journal of Neurophysiology*, *26*(6), 1003–1017. https://doi.org/10.1152/jn.1963.26.6.1003

Zhiling, Y., Fujita, E., Tanabe, Y., Yamagata, T., Momoi, T., & Momoi, M. Y. (2008). Mutations in the gene encoding CADM1 are associated with autism spectrum disorder. *Biochemical and Biophysical Research Communications*, *377*(3), 926–929. https://doi.org/10.1016/j.bbrc.2008.10.107